RESEARCH ARTICLE | FEBRUARY 19 2009

Thermal conductivity measurement of fluids using the 3ω method

Seung-Min Lee

Rev. Sci. Instrum. 80, 024901 (2009)
https://doi.org/10.1063/1.3082036

Thermal conductivity measurement of fluids using the 3ω method

Seung-Min Lee[a)]
Devices and Materials System Laboratory, LG Electronics Advanced Research Institute, Seoul 137-724, Republic of Korea

(Received 20 December 2008; accepted 25 January 2009; published online 19 February 2009)

We have developed a procedure to measure the thermal conductivity of dielectric liquids and gases using a steady state ac hot wire method in which a thin metal wire is used as a heater and thermometer. The temperature response of the heater wire was measured in a four-probe geometry using an electronic circuit developed for the conventional 3ω method. The measurements have been performed in the frequency range from 1 mHz to 1 kHz. We devised a method to transform the raw data into well-known linear logarithmic frequency dependence plot. After the transformation, an optimal frequency region of the thermal conductivity data was clearly determined as has been done with the data from thin metal film heater. The method was tested with air, water, ethanol, mono-, and tetraethylene glycol. Volumetric heat capacity of the fluids was also calculated with uncertainty and the capability as a probe for metal-liquid thermal boundary conductance was discussed. © *2009 American Institute of Physics.* [DOI: 10.1063/1.3082036]

I. INTRODUCTION

The 3ω method, a steady state ac method for thermal conductivity measurement, has been extensively applied by many groups.[1–12] Mostly a long and narrow thin metal film is used as a heater and thermometer so that the temperature oscillation at the heater typically exhibits linear logarithmic frequency dependence due to cylindrical heat diffusion outside the heater. The thermal conductivity of substrate appears in the linear coefficient of the logarithm of heating frequency. The thermal conductivity of films on substrate also can be extracted from a frequency independent shift from the thermal response of the bare substrate which can be measured separately.[3] In case the substrate has high thermal diffusivity, the temperature shift by the film dominates the substrate response so that we can use calculated substrate effect using the literature value of the heat capacity and the thermal conductivity.[4,5] About 200 nm thick metal film behaves as a perfect heat source because it generates precise Joule heating with almost indiscernible delay due to self-heating effect although the thermal conductance between the metal film and samples is not fully understood yet.[13–16]

On the other hand, the 3ω method using a long and thin metal wire has been restricted to a relatively few measurements.[7,11] One reason might be that there exist well established transient or steady state methods for gases and liquids.[17–19] Another reason would be the complexity of data analysis compared to film heater case. Many liquids and most gases have so low thermal conductivity that the self-heating of the metal wire is not negligible compared to heat flow into surrounding liquid or gas. Consequently the measured result does not show linear logarithmic frequency dependence. For air case, the effect appears even for heater wires of ~10 μm diameter. Although the heater heat capacity effect has been analytically explained,[7,11] the data analysis process is practically less intuitive than that of the metal film heater.

In this paper, we report a thermal conductivity measurement setup using a wire heater along with a new data analysis procedure. Using new procedure we could clearly locate the frequency region for valid analysis, which is of critical importance when we are unaware of the thermal property of a measuring fluid. The method has been tested with typical fluids including air, water, ethanol, mono-, and tetraethylene glycols.

II. EXPERIMENTAL

The electrical terminals for a thin heater wire and two voltage sensing wires were mounted on a printed circuit board (PCB), as shown in Fig. 1(a). To ease the handling of the wire mounted board, we have built an insert, as shown in Fig. 1(b). The four-probe geometry has been achieved as follows:

(1) Metal pins made of gold coated copper alloy[20] were soldered at positions (A, A', four C) or (B, B', four D) in Fig. 1(a).
(2) A gold heater wire between current feeding posts (A-A') and (B-B') was attached by winding and soldering. Care was taken to prevent the melting of thin gold wire.
(3) Another two gold wires of same diameter were attached between voltage sensing posts (C-C) and (D-D). At this time, to ensure a reliable electrical contact between heater wire and voltage sensing wires, we carefully wound gold wires of same diameter around the heater wire, as shown in Fig. 1(d). Due to excellent electrical contact property of gold, the contact resistance variation is almost negligible and no change has been noticed after two months.

Gold wires of 99.99% purity and 25 μm diameter (Ku-

a)Author to whom correspondence should be addressed. Electronic addresses: urbana@lge.com and urbanac@hanmail.net.

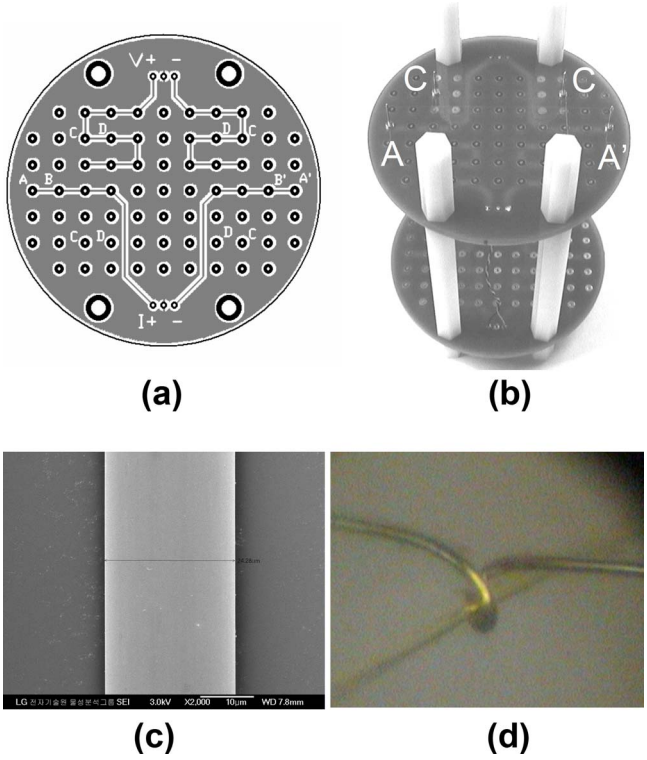

FIG. 1. (Color online) (a) PCB and electrical connection points. (b) Upside down photograph of the insert. Plastic stand offs are made of nylon. (c) SEM photo of a gold heater wire. The nominal value is 25 μm but the measured is 24.2 ± 0.2 μm. (d) Photo: voltage wire is wound around heater wire for reliable electrical contact.

licke & Soffa) or 99.9% purity and 12.7 μm in diameter (Alfa Aesar) were used for the heater. Using scanning electron microscopy (SEM) photos taken at two ends of 100 mm long wire, the diameter of the heater wire was measured as 24.2 ± 0.2 μm, which is about 3% smaller than the nominal value of 25 μm. The same gold wires were used for voltage sensing. In fact, chromel wires are better for voltage sensing because their thermal conductivity is much lower than gold wire so that heat leak along the voltage wire can be minimized. However, as we tested chromel wires (omega) of same diameter for voltage sensing, no appreciable difference was observed in the resulted thermal conductivity data. We have used two types of the four-probe geometry, as shown in Table I. The distance between the voltage probing point and voltage sensing post was 10 mm for both types.

To avoid the contamination of test fluid by PCB, the insert was cleaned using water-ethanol mixture. The insert was placed in laboratory glassware and later filled with small quantity of test fluid at the bottom. The electrical resistivity

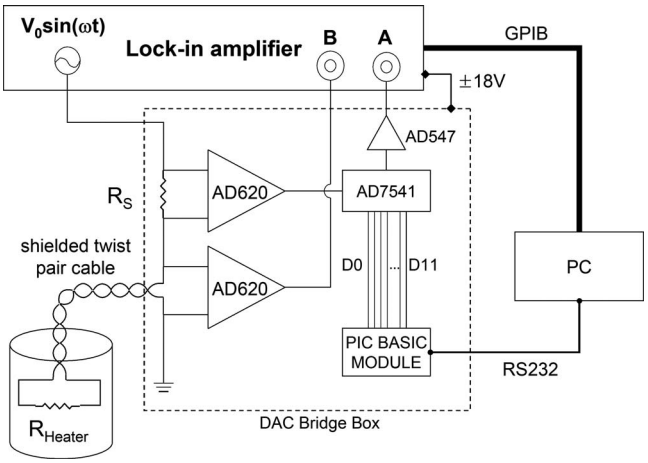

FIG. 2. Schematic of the electrical connection for automated data acquisition.

of de-ionized water was about 16 MΩ cm and the nominal purity of the ethanol and ethylene glycols was 99.9%.

The 3ω signals were collected using SRS830 lock-in amplifier (Stanford Research Systems) and DAC1220, a 12-bit multiplying digital-analog converter (MDAC) based bridge circuit.[1] Fig. 2 is the schematic of the electrical connections for signal process and instrument control. The measurement has been performed at seven points in the frequency range of 0.001–0.0105 Hz and 59 points in 0.0105–1000 Hz so that the measurement time usually took more than 24 h. The heating frequencies were selected at logarithmic spacing and the measurement has been done by a self-made program written in LABVIEW™. The program first calculates heating current from the ω voltage across the reference resistor of known value. Then the hot-wire resistance (R) is calculated from the ω voltage across the wire (V_1). After setting the multiplying DAC to make ω signals at A and B inputs of the lock-in amplifier, the 3ω voltage difference (V_3) between reference resistor and hot wire is measured to calculate the temperature oscillation amplitude of the heater as below,[1]

$$\Delta T = 2\frac{dT}{dR}\frac{R}{V_1}V_3. \quad (1)$$

We separately measured the temperature coefficient of the resistance of the gold wires as 0.003 40 K^{-1}. The experiment has been done in temperature and moist controlled environment but due to long measurement time at low frequencies, temperature uncertainty was 296.15 ± 1 K. To prevent slow absorption of water vapor or carbon dioxide by testing liquids, the measuring cell has been wrap sealed with poly-

TABLE I. Typical setting of four-probe geometry.

	Type I	Type II
Heater wire diameter	25 μm (nominal) 24.2 ± 0.2 μm (measured)	12.7 μm (nominal) 14.8 ± 0.1 μm (measured)
Heater wire length	50 mm	40 mm
Voltage probing point distance	30 mm	20 mm

mer film. At frequencies below 0.01 Hz, the data stabilization time extends over several hours due to low pass filter of the lock-in amplifier. Instead of waiting sufficiently long time of ~100 times the heating period, the filter time constant has been set to at least ten times the heating period and the lock-in amplifier outputs were read and stored to series of data files at every second. Last five heating cycle data were taken and the modal value was chosen as data point at the frequency.

III. DATA REDUCTION

Due to heat capacity of the heater wire, the 3ω signal behaves much different from those by narrow metal film heaters. Assuming cylindrical symmetry of heat diffusion, the analytic solution of the temperature inside and outside the heater wire has been reported as[7,11]

$$T(r) = \begin{cases} AI_0\left(\sqrt{\frac{2i\omega C_h}{\kappa}}r\right) + \frac{P}{2i\omega C_h \pi r_0^2 L} & (r \le r_0) \\ BK_0\left(\sqrt{\frac{2i\omega C}{\Lambda}}r\right) & (r \ge r_0) \end{cases},$$

where C, Λ are the volumetric heat capacity and thermal conductivity of the test fluid; ω is the angular frequency of the heating current; r_0, L, C_h, κ are the radius, length, volumetric heat capacity, and thermal conductivity of the heater wire, respectively; P is the ac heating power of the heater wire; and $I_0(z)$, $K_0(z)$ are the zeroth order modified Bessel functions of the first and the second kind, respectively.

The continuity conditions of temperature and heat flux at $r=r_0$ give

$$A = \frac{P}{2i\omega C_h \pi r_0^2 L} \frac{1}{\frac{i\omega C_h r_0}{\Lambda\sqrt{\frac{2i\omega C}{\Lambda}} K_1\left(\sqrt{\frac{2i\omega C}{\Lambda}} r_0\right)} K_0\left(\sqrt{\frac{2i\omega C}{\Lambda}} r_0\right) + I_0\left(\sqrt{\frac{2i\omega C_h}{\kappa}} r_0\right)}$$

and

$$B = \frac{P}{2i\omega C_h \pi r_0^2 L} \frac{1}{K_0\left(\sqrt{\frac{2i\omega C}{\Lambda}} r_0\right) + \frac{\Lambda\sqrt{\frac{2i\omega C}{\Lambda}} K_1\left(\sqrt{\frac{2i\omega C}{\Lambda}} r_0\right)}{i\omega C_h r_0} I_0\left(\sqrt{\frac{2i\omega C_h}{\kappa}} r_0\right)}.$$

Taking average of the temperature inside the heater wire and adding possible thermal boundary effect, the 3ω signal can be generalized as follows:

$$\Delta T(\omega) \cong \frac{1}{\frac{\sqrt{\frac{2i\omega C}{\Lambda}} r_0 K_1\left(\sqrt{\frac{2i\omega C}{\Lambda}} r_0\right)}{\frac{P}{2\pi\Lambda L} K_0\left(\sqrt{\frac{2i\omega C}{\Lambda}} r_0\right)} + \frac{2i\omega C_H}{P}} + \frac{P}{8\kappa\pi L} + \frac{R_T P}{2\pi r_0 L}. \quad (2)$$

$\Delta T(\omega)$ is the measured in-phase and out-of-phase temperature oscillation of heater wire expressed as complex number. R_T is the thermal boundary resistance (TBR) between the heater metal and the fluid. $K_1(z)$ is the first order modified Bessel functions of second kind and $C_H \equiv \pi r_0^2 L C_h$. The first term in fractional form is the combined thermal response of heater heating and diffusion by the fluid. The second term is the offset due to temperature profile inside the heater wire while the third term is the thermal boundary effect. Since we use gold wire of high thermal conductivity, the second term is negligible. The third term may be considerable depending on the TBR at gold heater-fluid interface but we may start with neglecting the effect.

Equation (2) results in a variety of $\Delta T(\omega)$ curves depending on the measurement condition such as thermal conductivity of the testing fluid, the heater heat capacity, and the heater diameter. The data for room air measured by free-standing heater wire is shown in Fig. 3 as an example. A relaxationlike peak in the out-of-phase data is mainly due to the heater heat capacity. For liquids, however, data did not show such peak because the heat diffusion into the liquid dominates the self-heating of the heater wire. As previously reported,[7,11] the measured data may be fitted by adjusting the parameters C, Λ, and C_H of Eq. (2). r_0, L are usually fixed to

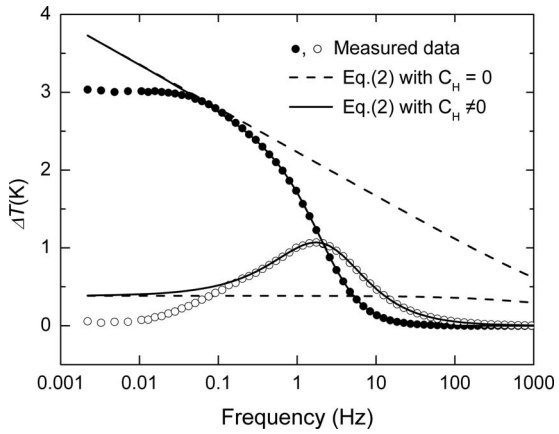

FIG. 3. In-phase (●) and out-of-phase (○) temperature oscillations of room air as measured using type I setup in a capped enclosure. Fitting lines are from Eq. (2) with and without heat capacity of heater wire (C_H) and Λ_{air} =0.026 W/K m, C_{air}=1.31 kJ/m^3 K. The effect of R_T is neglected.

measured values but one may adjust slightly to better fit the data. Practically, the heater wire is not a perfect cylindrical shape and it is hard to measure the wire diameter within 5% accuracy without SEM photos. The parameters might be optimized by doing numerical calculations starting with previously reported values of similar material as initial values.

The fitting process can be performed manually or by automated optimization algorithms based on least squares error sum method. But such process seriously depends on the input data which usually contain neglected effects such as heat leaks along the heater or onset of convection at low frequency measurement as well as decreased third harmonic voltage and phase shift by the read-out circuit at high frequency measurements. In Fig. 3, we also plotted curves of Eq. (2) assuming two cases of $C_h=0$ and $C_h=2.54\times10^6$ J/m^3 K. As shown, the fitting was successful only for a specific range of the heater frequency. Although the deviation at low frequency regions may be qualitatively explained by the heat leaks along the heater wire, as far as we know, analytic modification to Eq. (2) is not available at present due to three dimensional effect of such heat leak. Therefore it is hard to reason the validity of arbitrarily selected frequency region for data fitting process.

In this work we introduce a relatively simple way of data manipulation process with improved reasoning of the valid region for the thermal conductivity calculation as follows:

Step 1. Convert the voltage data into temperature data $\Delta T(\omega)$ using Eq. (1). Then subtract the second and the third terms in Eq. (2), which was skipped at first. Setting $z=\sqrt{2i\omega C/\Lambda}r_0$,

$$S_1(\omega) \equiv \Delta T - \frac{P}{8\kappa\pi L} - \frac{R_T P}{2\pi r_0 L} = \frac{1}{\dfrac{zK_1(z)}{\dfrac{P}{2\pi\Lambda L}K_0(z)} + \dfrac{2i\omega C_H}{P}}.$$

Step 2. Take the inverse of $S_1(\omega)$.

$$S_2(\omega) \equiv \frac{1}{S_1(\omega)} = \frac{zK_1(z)}{\dfrac{P}{2\pi\Lambda L}K_0(z)} + \frac{2i\omega C_H}{P}.$$

Step 3. Subtract the second term of $S_2(\omega)$ and inverse the result.

$$S_3(\omega) \equiv \frac{1}{S_2(\omega) - \dfrac{2i\omega C_H}{P}} = \frac{P}{2\pi\Lambda L}\frac{K_0(z)}{zK_1(z)}.$$

Step 4. We define one complex and two real functions,

$$G(z) \equiv \frac{K_0(z)}{zK_1(z)},$$

$$f(\omega) \equiv \frac{\mathrm{Im}[S_3(\omega)]}{\mathrm{Re}[S_3(\omega)]}, \quad g(z) \equiv \frac{\mathrm{Im}[G(z)]}{\mathrm{Re}[G(z)]}.$$

Then

$$S_3(\omega) = \frac{P}{2\pi\Lambda L}G(z)$$

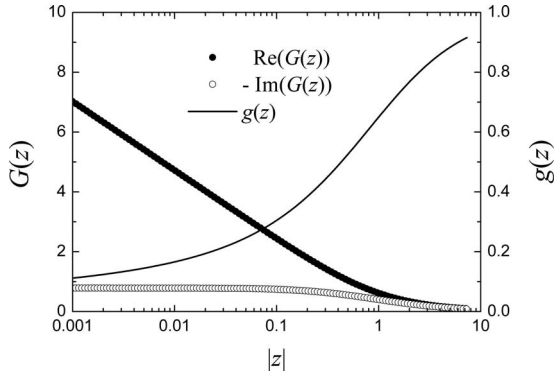

FIG. 4. Numerical function plot of $G(z)=K_0(z)/zK_1(z)$ and $g(z)=\mathrm{Im}[G(z)]/\mathrm{Re}[G(z)]g(z)$ is monotonic at least for the shown region of $0.001<|z|<10$.

and

$$f(\omega) = \frac{\mathrm{Im}\left[\dfrac{K_0(z)}{zK_1(z)}\right]}{\mathrm{Re}\left[\dfrac{K_0(z)}{zK_1(z)}\right]} = g(z).$$

Note that $f(\omega)$ is calculated from the measured data while $g(z)$ is an analytic function of z. Since $g(z)$ is monotonic in $|z|$, as shown in Fig. 4, a unique z can be obtained for each ω taking the inverse function of g; $z=g^{-1}[f(\omega)]$. Practically, instead of analytically solving for inverse function, we tabulate the numerical values of $g((1+i)|z|/\sqrt{2})$ for $0.001\le|z|\le10$ and interpolate the $|z|$ value satisfying $g(z)=f(\omega)$.

Step 5. Using z obtained in the step 4, we calculate $zK_1(z)$ and multiply it to $S_3(\omega)$.

$$S_5(\omega) \equiv zK_1(z)S_3(\omega) = \frac{P}{2\pi\Lambda L}K_0\left(\sqrt{\frac{2i\omega C}{\Lambda}}r_0\right). \tag{3}$$

Now that Eq. (3) has frequency dependence similar to those by a thin metal film heater, the thermal conductivity (Λ) of the test fluid can be obtained from a linear fit to the reduced data as has been done with metal film heater.

Since $K_0(z)\cong-\ln z+\ln 2-\gamma$, where $\gamma\sim0.5772$ as $|z|$ approaches 0, the thermal conductivity (Λ) of the test fluid can be calculated as follows:

$$\frac{1}{\Lambda} = -\frac{4\pi L}{P}\frac{d}{d\ln\omega}S_5(\omega). \tag{4}$$

We note that the relation of $S_5(\omega)=P/2\pi\Lambda LK_0(\sqrt{2i\omega C/\Lambda}r_0)$ is satisfied in a specific frequency range due to effects not considered in Eq. (2). For example, if we use thick wires for low thermal diffusivity sample, the frequency range becomes so narrow that it is hard to set the fitting region. For this reason, our data transformation steps are advantageous in considering the validity of fit parameters. As a demonstration, intermediate results after steps 3 and 5 are compared in Figs. 5–7. Another great advantage of the explained transformation is that the thermal conductivity can be obtained by a linear fit which can be automated easily

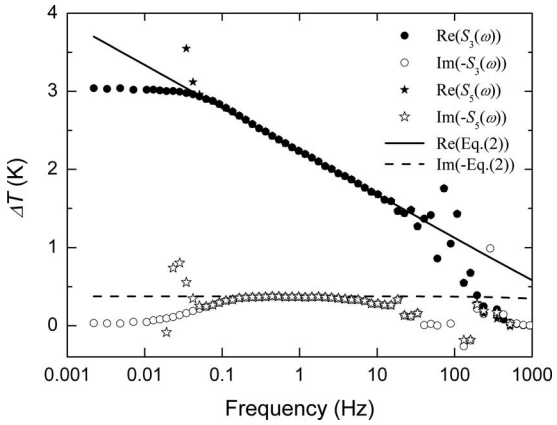

FIG. 5. Room air data after steps 3 and 5: deviations below 0.1 Hz and scatterings above 10 Hz are due to measurement resolution related to both the dynamic range of data acquisition and the environment noise. Data between 0.25 and 8.4 Hz were used for calculation of $\Lambda=0.0265$ W/K m.

for series of data obtained by time dependent or temperature dependent measurements. The transformation steps were written in LABVIEW™ so that the parameter fittings and the frequency region selection for thermal conductivity calculation can be done interactively. The program was further modified to handle temperature or time dependent measurement data by enabling the setting of different frequency windows for each temperature or time.

IV. RESULTS AND DISCUSSIONS

In Figs. 5–8 we show the data for air, de-ionized water, ethanol, mono-, and tetraethylene glycol. All the data were obtained by the same hot wire insert of type I and the actual temperature amplitude is shown in the figures. Except for the air case, the heating power has been kept as low as the temperature amplitude of the heater was <1 K in the measured frequency region. The heating power was 0.31–0.32 W/m for liquids. The heating power was different for each liquid since the dc temperature of the heater was slightly dependent on the thermal diffusivity of the liquids. For air case we tested with two different power levels of 0.08 and 0.02 W/m which correspond to 3 and 0.8 K heating. Data for 0.02 W/m heating showed lower signal-to-noise ratio than for 0.08 W/m heating but the calculated thermal conductivity value did not show significant difference of the estimates.

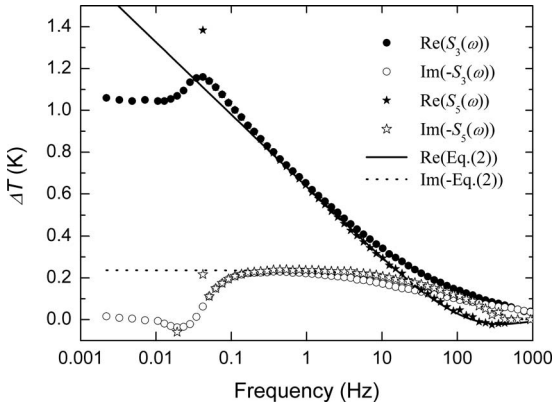

FIG. 7. Ethanol: fitting lines are Eq. (2) with $\Lambda=0.170$ W/K m, $C=1.71\times10^6$ J/m^3 K. Data between 0.44 and 22.4 Hz were used for calculation of Λ.

The thermal conductivity of the test fluids was calculated using the relation of Eq. (4). For linear fit to thermal conductivity, different frequency regions were selected for each fluid. We note that the imaginary part of $S_5(\omega)$ shows wider flat region than that of $S_3(\omega)$, which facilitates the visual selection of frequency region for thermal conductivity calculation. Although we might use data at two different frequencies to average out system noise, we used linear fitting against $\ln(\omega)$ in a frequency region. Since $S_5(\omega)$ deviated from $-\ln(\omega)$ curve both at low and at high frequencies, the selection of the lower and upper frequencies for thermal conductivity calculation considerably affected the data. Therefore we set f_L as the frequency where $-\mathrm{Im}[S_5(\omega)]$ starts to decrease and f_U where $\mathrm{Re}[S_5(\omega)]=-\mathrm{Im}[S_5(\omega)]$. For the case of air, f_U was much higher than the measurement range but we set f_U as the highest frequency without serious data scattering. Then, we gradually narrow the window for which thermal conductivities were calculated by least squares error fitting. The median of the series of calculated values $(\Lambda_k, 1\leq k\leq \frac{1}{2}N)$ for N frequencies in $f_L\leq f\leq f_U$ was selected as the thermal conductivity of the fluid. We used median value because average value is more sensitive to system noise and

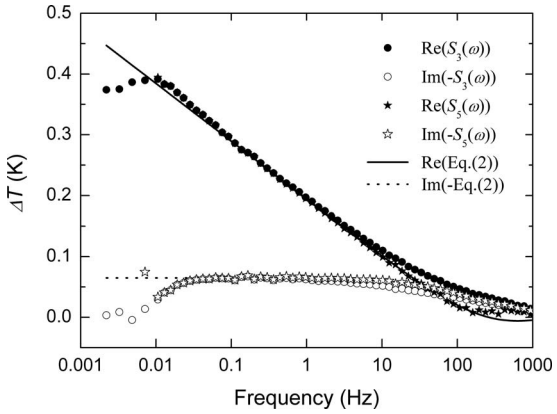

FIG. 6. De-ionized water: fitting lines are Eq. (2) with $\Lambda=0.610$ W/K m, $C=3.77\times10^6$ J/m^3 K. Data between 0.05 and 33.2 Hz were used for calculation.

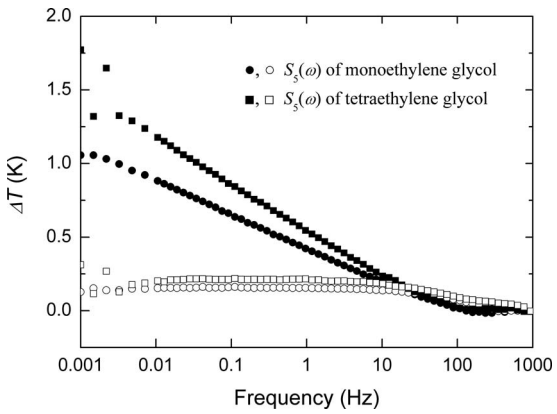

FIG. 8. (a) Monoethylene glycol: data between 0.034 and 18.4 Hz were used for calculation of $\Lambda=0.256$ W/K m. (b) Tetraethylene glycol: data between 0.019 and 18.4 Hz gave $\Lambda=0.184$ W/K m.

TABLE II. Measured thermal conductivity and volumetric heat capacity.

Test fluids	f_L, f_U(Hz) (N=data points)	Λ(W/K m) This work	Λ(W/K m) Literature	$C(\times 10^6$ J/K m$^3)$ This work	$C(\times 10^6$ J/K m$^3)$ Literature
Air	0.25, 8.4 (N=19)	0.0265 ±0.0003	0.0262[a]	0.00168 ±0.0002	0.001 31
De-ionized water	0.05, 33.2 (N=34)	0.610 ±0.02	0.610[b]	3.77 ±0.49	4.18[c]
Ethanol	0.44, 22.4 (N=21)	0.170 ±0.005	0.162[d] 0.171[e]	1.708 ±0.116	1.935[c]
Monoethylene glycol	0.034, 18.4 (N=33)	0.256 ±0.002	0.254[f]	2.523 ±0.068	2.691[c]
Tetraethylene glycol	0.019, 18.4 (N=36)	0.184 ±0.002	0.188[g]	2.185 ±0.092	2.444[c]

[a]At 300 K, Ref. 21.
[b]At 300 K, Ref. 22.
[c]At 300 K, Ref. 26.
[d]At 303.15 K, Ref. 23.
[e]At 298.15 K, Ref. 24.
[f]At 298.6 K, Ref. 25.
[g]At 296.5 K, Ref. 24. See text for the listed standard deviations of the measured thermal conductivity and heat capacity.

end points selection. Data were compared with the literature values, as shown in Table II. All the data were in good agreement with literature values except for tetraethylene glycol. The standard deviations of Λ_k and N were also listed in the table to show the reliability of the process.

As was attempted previously,[27,28] we also calculated the volumetric heat capacity of the test fluids. If we neglect the TBR between heater and fluid, heat capacity of fluids can be calculated from $S_5(\omega)$ as

$$C = \frac{\Lambda}{2i\omega r_0^2}\exp\left[-\frac{4\pi\Lambda L}{P}S_5(\omega) - 2\ln 2 + 2\gamma\right].$$

Alternatively we may use only the real part of $S_5(\omega)$ so that

$$C = \frac{\Lambda}{2\omega r_0^2}\exp\left\{-\frac{4\pi\Lambda L}{P}\mathrm{Re}[S_5(\omega)] - 2\ln 2 + 2\gamma\right\}. \quad (5)$$

We took the average of the calculated values of C between f_L and f_U. The uncertainty of Λ influences that of C as

$$\delta C/C = \left\{1 - \frac{4\pi L\Lambda}{P}\mathrm{Re}[S_5(\omega)]\right\}\delta\Lambda/\Lambda,$$

which dominates the standard deviations of Eq. (5) evaluated for data between f_L and f_U. We listed the root mean square of δC in Table II.

We may attribute the serious deviation of calculated heat capacity (ΔC) from the literature values in Table II to TBR (R_T) between heater and test fluids. Equation (2) can be rewritten as

$$\Delta T(\omega) \approx \frac{1}{\dfrac{1}{S_5(\omega)} + \dfrac{2i\omega C_H}{P}} + \frac{P}{8\kappa\pi L} + \frac{R_T P}{2\pi r_0 L}$$

so that the uncertainty of $R_T P/2\pi r_0 L$ results in

$$\Delta S_5(\omega) \sim \frac{R_T P}{2\pi r_0 L}$$

and

$$\Delta C/C = 1 - \exp\left(\frac{4\pi\Lambda L}{P}\frac{R_T P}{2\pi r_0 L}\right) \sim -\frac{2\Lambda R_T}{r_0}. \quad (6)$$

Equation (6) indicates that the ratio between the boundary thermal conductance and the fluid thermal conductivity is the error factor. For example, Λ=0.3 W/K m, R_T =10^{-8} K m^2/W, and $2r_0$=25 μm gives about 0.05% error in C. The error becomes serious for highly conductive test fluid, very thin heater wire, and high TBR. In reverse, we may discuss the capability of the present method as a probing tool for the TBR between heater metal and test fluids. Equation (2) implies that we may calculate R_T if we know the heat capacity of the measuring fluid. Equation (6) can be rewritten as $\delta R_T \sim r_0 \delta C/2\Lambda C$, where δR_T and δC are the accuracy of calculated R_T and the C of the measuring fluid, respectively. For example, the accuracy of R_T between gold and a liquid of Λ=0.3 W/K m using 25 μm diameter wire is about 2×10^{-7} K m^2/W with 1% accuracy of C value. For 25 μm diameter gold wire, the second term in Eq. (2) corresponds to the third term with R_T =10^{-8} K m^2/W, which is comparable to reported TBR at dielectric-metal interfaces.[4,5,14–16] Although we assume the smallest difference from the literature values of C, $R_T > 5\times 10^{-7}$ K m^2/W was estimated from the data of ethanol and ethylene glycols. We suspect imperfections such as roughness and particulates on the surface of gold wire and intrinsic resistance as the origin of TBR.

Below 0.1 Hz, the real parts of the data for liquids show slight rise above Eq. (2) and approach constant value at lowest measured frequency. Since the behavior was observed sensitive to heating power, we suspect that static temperature gradient induced convection is related to the slight rise.

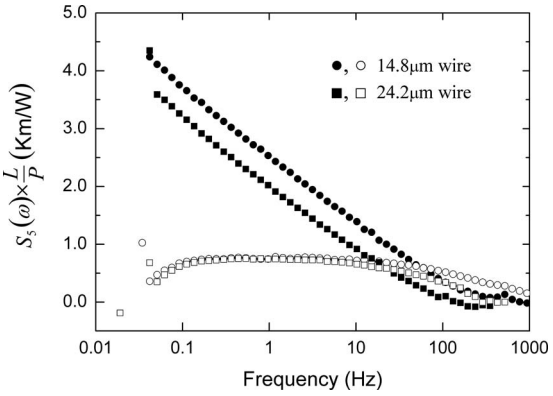

FIG. 9. Data for ethanol with two different heater wire diameters. The temperature is normalized by heating power per length. Note that slopes of the real part are the same and frequency dependence of the thicker diameter is shifted to lower frequency.

Above 0.1 Hz, in this experiment, the heat transport was dominated by the conduction of the fluid so that the effect of convection was more prominent than in the case of using microscale heater film on solid substrate or membrane.[29] For air case, data show saturation with hardly noticeable peak. On the other hand, the imaginary parts approach zero as frequency decreases, which can be explained by dominant heat conduction along the heater wire and voltage sensing wires. We note that the overall frequency dependence of our measurements is different from the work of Lu *et al.*[30] where radial heat diffusion is absent due to vacuum environment. Since the saturation values at lowest frequency depend on the ratio among the heat flows along the heater and the voltage probing wire and into the test fluid, the value may be used for the thermal conductivity of the test fluid. However, the method is not recommended considering the long data acquisition time and complicated convection effect as well as large thermal conductivity addendum by heater metal. Although the test fluids were wrap sealed and placed inside heat insulated metal shield box, data showed slow variations. For seven repetitions of measurement with ethanol, the standard deviation of the thermal conductivity was 0.000 28 W/K m. Such a deviation is much smaller than heater length measurement error which is at most 5% if we consider the incomplete straightness of the wire as well as the length measurement error of about 50 μm.

We have performed measurement using 14.8 ± 0.1 μm wire (nominally 12.7 μm wire) but observed no significant difference in the calculated thermal conductivity. Data for ethanol with different wire diameter are shown in Fig. 9. We applied different heating powers to keep the same temperature amplitude to avoid different temperature distributions for two wire diameters and plot the temperature amplitude per linear heating power to help the comparison of the data. The diameter difference exhibits only a frequency shift as predicted from Eq. (3). Such an agreement implies that calibration with standard fluid is not necessary if only we know the wire diameter.

ACKNOWLEDGMENTS

The author thanks Professor D. G. Cahill for helpful advice.

[1] D. G. Cahill, Rev. Sci. Instrum. **61**, 802 (1990).
[2] Y. H. Jeong and I. K. Moon, Phys. Rev. B **52**, 6381 (1995).
[3] S.-M. Lee, D. G. Cahill, and T. H. Allen, Phys. Rev. B **52**, 253 (1995).
[4] S.-M. Lee and D. G. Cahill, J. Appl. Phys. **81**, 2590 (1997).
[5] J. H. Kim, A. Feldman, and D. Novotny, J. Appl. Phys. **86**, 3959 (1999).
[6] Y. S. Ju, K. Kurabayashi, and K. E. Goodson, Thin Solid Films **339**, 160 (1999).
[7] N. O. Birge, Phys. Rev. B **34**, 1631 (1986).
[8] T. Borca-Tasciuc, A. R. Kumar, and G. Chen, Rev. Sci. Instrum. **72**, 2139 (2001).
[9] A. Jacquot, B. Lenoir, A. Dauscher, M. Stölzer, and J. Meusel, J. Appl. Phys. **91**, 4733 (2002).
[10] T. Yamane, Y. Mori, S. Katayama, and M. Todoki, J. Appl. Phys. **91**, 9772 (2002).
[11] F. Chen, J. Shulman, Y. Xue, C. W. Chu, and G. S. Nolas, Rev. Sci. Instrum. **75**, 4578 (2004).
[12] B. W. Olson, S. Graham, and K. Chen, Rev. Sci. Instrum. **76**, 053901 (2005).
[13] A. Majumdar and P. Peddy, Appl. Phys. Lett. **84**, 4768 (2004).
[14] Y. S. Ju, M.-T. Hung, M. J. Carey, M.-C. Cyrille, and J. R. Childress, Appl. Phys. Lett. **86**, 203113 (2005).
[15] H.-C. Chien, D.-J. Yao, M.-J. Huang, and T.-Y. Chang, Rev. Sci. Instrum. **79**, 054902 (2008).
[16] R. M. Costescu, D. G. Cahill, F. H. Fabreguette, Z. A. Sechrist, and S. M. George, Science **303**, 989 (2004).
[17] P. Andersson and G. Bäckström, Rev. Sci. Instrum. **47**, 205 (1976).
[18] Y. Nagasaka and A. Nagashima, Rev. Sci. Instrum. **52**, 229 (1981).
[19] J. D. Raal and R. L. Rijdsijk, J. Chem. Eng. Data **26**, 351 (1981).
[20] Advanced Interconnections Corp., http://www.advanced.com.
[21] K. Stephan and A. Laesecke, J. Phys. Chem. Ref. Data **14**, 227 (1985).
[22] M. L. V. Ramires, C. A. Nieto de Castro, Y. Nagasaka, A. Nagashima, M. J. Assael, and W. A. Wakeham, J. Phys. Chem. Ref. Data **24**, 1377 (1995).
[23] L. Qun-Fang, L. Rui-Sen, N. Dan-Yan, and H. Yu-Chun, J. Chem. Eng. Data **42**, 971 (1997).
[24] J. D. Raal and R. L. Rijsdijk, J. Chem. Eng. Data **26**, 351 (1981).
[25] R. DiGuilio and A. S. Teja, J. Chem. Eng. Data **35**, 117 (1990).
[26] M. Zábranský, V. Růžička, Jr., V. Majer, and E. S. Domalski, J. Phys. Chem. Ref. Data Monograph No. 6 **1**, 283 (1996).
[27] S.-M. Lee and S.-I. Kwun, Rev. Sci. Instrum. **65**, 966 (1994).
[28] S. R. Choi, J. Kim, and D. Kim, Rev. Sci. Instrum. **78**, 084902 (2007).
[29] X. J. Hu, A. Jain, and K. E. Goodson, Int. J. Therm. Sci. **47**, 820 (2008).
[30] L. Lu, W. Yi, and D. L. Zhang, Rev. Sci. Instrum. **72**, 2996 (2001).